1990ApJ...355...52E

THE ASTROPHYSICAL JOURNAL, 355:52–58, 1990 May 20
© 1990. The American Astronomical Society. All rights reserved. Printed in U.S.A.

OPTICAL TRACERS OF SPIRAL WAVE RESONANCES IN GALAXIES: APPLICATIONS TO NGC 1566

BRUCE G. ELMEGREEN[1] AND DEBRA MELOY ELMEGREEN[2]

Received 1989 August 4; accepted 1989 November 17

ABSTRACT

Likely radii for the inner and outer Lindblad resonances (ILR, OLR), the corotation resonance (CR), the inner 6:1 and 4:1 resonances, and the outer 1:1 resonance in the grand design galaxy NGC 1566 are identified from optical features and from constraints set by plausible rotation curves. In the preferred solution, the OLR is placed where the outer edge of the spiral pattern joins the outer ring, the CR is at the endpoints of the bright star-formation ridges and sharply defined dust lanes, where the main arms bifurcate and a ring of interarm star-formation circles the galaxy, the 6:1 resonance is where two short and faint spurs lie parallel and equally spaced between the main arms in the west, the 4:1 resonance is where a large and bright spur lies midway between the arms in the east and where there is a kink in both arms, and the ILR is at the position of another kink in the spiral at the inner part of the galaxy, near the end of a small bar. The outer ring extends between the OLR and the outer 1:1 resonance. The ratios of these resonance radii to the corotation resonance are shown to be relatively insensitive to the rotation curve, and all of the observed ratios are in good agreement with theory. Other possible solutions for the resonance radii are discussed.

Subject headings: galaxies: individual (NGC 1566) — galaxies: internal motions — galaxies: structure

I. INTRODUCTION

According to the modal theory of galactic spiral structure (Bertin *et al.* 1989 and references therein) and the nonlinear orbit theory (Contopolous and Grosbøl 1986, 1988), quasi-stationary spiral wave patterns interact with stars and gas in specific and predictable ways at the primary orbit resonances, which include: the corotation resonance, the ultraharmonic or 4:1, 6:1, etc. resonances, the inner Lindblad resonance (ILR), and the outer Lindblad resonance (OLR). Considerable effort has been spent trying to locate these resonances in galaxies. Although Lin and Shu (1967) suggested that galactic spirals should exist primarily between the inner and outer Lindblad resonances, a consensus seemed to emerge following Roberts (1969) and Roberts, Roberts, and Shu (1975), that corotation, rather than the OLR, should be near the optical edge of the disk. This followed from the assumption that star formation should occur primarily where there is a strong shock, which is inside the corotation radius. This idea was reinforced by the proposal that a barrier to wave propagation exists at the corotation resonance for disks with reasonably large stability parameters, $Q > 1$ (Toomre 1977). Further limitations came from numerical simulations (Contopoulos and Grosbøl 1986, 1988) which showed that the stars do not reinforce an imposed spiral potential beyond the inner 4:1 resonance, which typically lies at only 60% of the corotation radius. All of these studies offered prescriptions for determining the corotation radius and, therefore, the spiral pattern speed, from the optical morphology (i.e., the galaxy edge). There were no independent kinematic checks for the proposed pattern speeds however, nor were there any attempts to fit all of the main resonances simultaneously to specific morphological features, given the constraints set by the rotation curve.

Several years ago, some of the basic assumptions used for these pattern speed determinations became suspect. The connection between star formation and density waves grew less obvious than originally thought (Elmegreen 1985; Elmegreen and Elmegreen 1986; McCall and Schmidt 1986; Elmegreen 1987*a*), to the extent that detailed observations showed comparable rates of star formation whether or not there was a spiral (e.g., Hunter and Gallagher 1986; Thronson *et al.* 1989). Star formation proceeds wherever the column density or density of gas are sufficiently high (Guiderdoni 1987; Kennicutt 1989); large-scale shocks, if they occur in a galaxy, directly trigger only part of the total star formation. Moreover, the concept that stellar waves cannot penetrate beyond the corotation resonance now seems to depend strongly on the assumed role of gas, both as a means of dissipating energy and as an additional mass for wave forcing (Shu 1985; Lubow 1986; Bertin *et al.* 1989). Indeed, modal solutions by Bertin *et al.* (1989) show corotation midway out in the spiral, sometimes at the radius of a local maximum in the spiral density response. The additional limitation imposed by the lack of a sufficiently organized stellar response beyond the 4:1 resonance also seems to depend strongly on the presence of gas, as well as the spiral arm strength (Grosbøl 1989). Thus we can no longer assume that corotation is at or beyond the edge of the visible disk.

Morphological methods for locating resonances in galaxies are still the most promising, in view of the persistent difficulty in determining galactic pattern speeds directly, from kinematic data for example (e.g., Tremaine and Weinberg 1984; Kent 1987). Such a morphological study was recently attempted for the three most regular and symmetric of the nearby spiral galaxies, M51, M81, and M100 (Elmegreen, Elmegreen, and Seiden 1989; hereafter EES). In each case, all four primary resonances (ILR, 4:1, CR, OLR) could be associated in a unique way, considering the rotation curves, with clear and sensible optical features. This result suggests that some orbit resonances appear as recognizable features in galaxies, such as spiral arm kinks, gaps, spurs, bifurcations, and endpoints, as well as endpoints to star-formation ridges, dust lane cross-over points, and interarm star formation. When a large number of

[1] IBM Research Division, T. J. Watson Research Center.
[2] Vassar College Observatory, Poughkeepsie, NY.

© American Astronomical Society • Provided by the NASA Astrophysics Data System

1990ApJ...355...52E

resonances is matched by such features in a symmetric galaxy, the pattern speed would seem to be reasonably certain.

Unfortunately, very few galaxies are as symmetric and well studied as M51, M81 and M100. There are few detailed optical and kinematic studies of other low inclination grand design galaxies because such galaxies are rare, and similar morphological analyses of multiple arm galaxies, which are more common, may be difficult to interpret if these galaxies have more than one pattern speed (Elmegreen 1989; Lin and Lowe 1989). Perhaps other methods for locating CR resonances can be applied to these cases (e.g., Cepa and Beckman 1990).

Here we consider the morphology of NGC 1566, which is a grand design galaxy illustrated in Sandage and Bedke (1988; hereafter SB) that exhibits many of the same resonance features as M51, M81 and M100. NGC 1566 is a weakly barred, SAB(s)bc type galaxy with bright spiral arms that extend halfway out in the disk, spurs that branch from the main arms at diametrically opposite locations, sharply defined dust lanes on the inner edges of the arms, and a faint outer arm or ring-like structure that extends to approximately R_{25}, the 25th magnitude per arcsec^2 isophotal radius. Giant patches of star formation trace the inner arms downstream from the dust lane (Comte and Duquennoy 1982; Roy, Belley, and Walsh 1989), suggesting that the density wave initiated the formation of superclouds and giant star clusters (Elmegreen and Elmegreen 1983).

The optical morphology of NGC 1566 is similar to that of M51, M81, and M100. In our resonance fits for M100 and M51, which consider both morphology and rotation curves, the inner ovals terminate at the inner Lindblad resonances, bright star-forming ridges and dust lanes end at the corotation resonances, and the main spirals end at the outer Lindblad resonances. M81 and M100 also contain inner reflection points for the main stellar waves, so the stellar waves are shielded from the inner Lindblad resonances, and the 4:1 resonances are highlighted by spurs 90° away from the main arms on each side. Prominent interarm star formation also occurs at the corotation resonance in M100, possibly the result of local gravitational instabilities that operate independently of the wave (Elmegreen 1987*b*). M51 differs from M100 in not having an obvious inner reflection point (the main stellar wave apparently extends all the way to the oval in the center), and M51 also has an outer material arm (e.g., Howard and Byrd 1990).

The morphological similarities between M51, M81, M100, and NGC 1566 suggest that the orbital resonances in NGC 1566 may be determined from optical features analogous to those in M100 and M51. Here this hypothesis is shown to be consistent with likely rotation curves.

II. RESONANCE-TYPE FEATURES IN NGC 1566

A deprojected image of NGC 1566, with the average radial profile subtracted, and an azimuth versus log-radius plot of the image, made in the manner discussed in EES, are shown in Figure 1 (Plate 1). The original digitized image was taken from the SB atlas using a video camera. The length of the calibration bar on the right in the galaxy image is the radius at a surface brightness of 25 mag per arcsec^2, R_{25}, equal to 3.'88 from D_0 in de Vaucouleurs, de Vaucouleurs, and Corwin (1976). The calibration bar on the left represents 100 pixels. The tic marks on the vertical axis of the azimuth versus log-radius plot are in units of 0.1 R_{25}, from 0.1 R_{25} to 0.9 R_{25}. The marks on the horizontal axis are at $-180°$, 0°, 180°, 360°, and 540° measured around the galaxy center counter-clockwise from the major axis on the north side (north is left on page 33 in SB and north is approximately to the right in Fig. 1, so the $-180°$ position on the log R vs. θ diagram is to the left on the top figure). The average pitch angle of the spiral arms is determined from this latter plot to be $\sim 24°$, in agreement with Sersic and Calderon (1978) and Kennicutt (1981). Deprojection

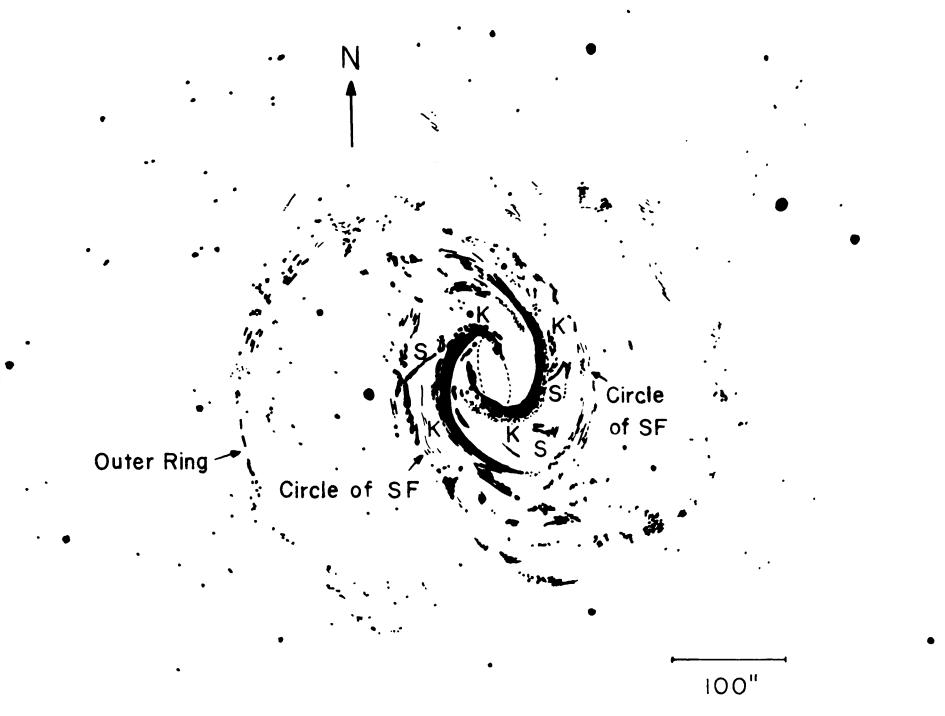

FIG. 2.—Sketch of NGC 1566, from Sandage and Bedke (1988; p. 43), showing features discussed in the text. The symbols "S" and "K" represent spurs and kinks, respectively.

© American Astronomical Society • Provided by the NASA Astrophysics Data System

1990ApJ...355...52E

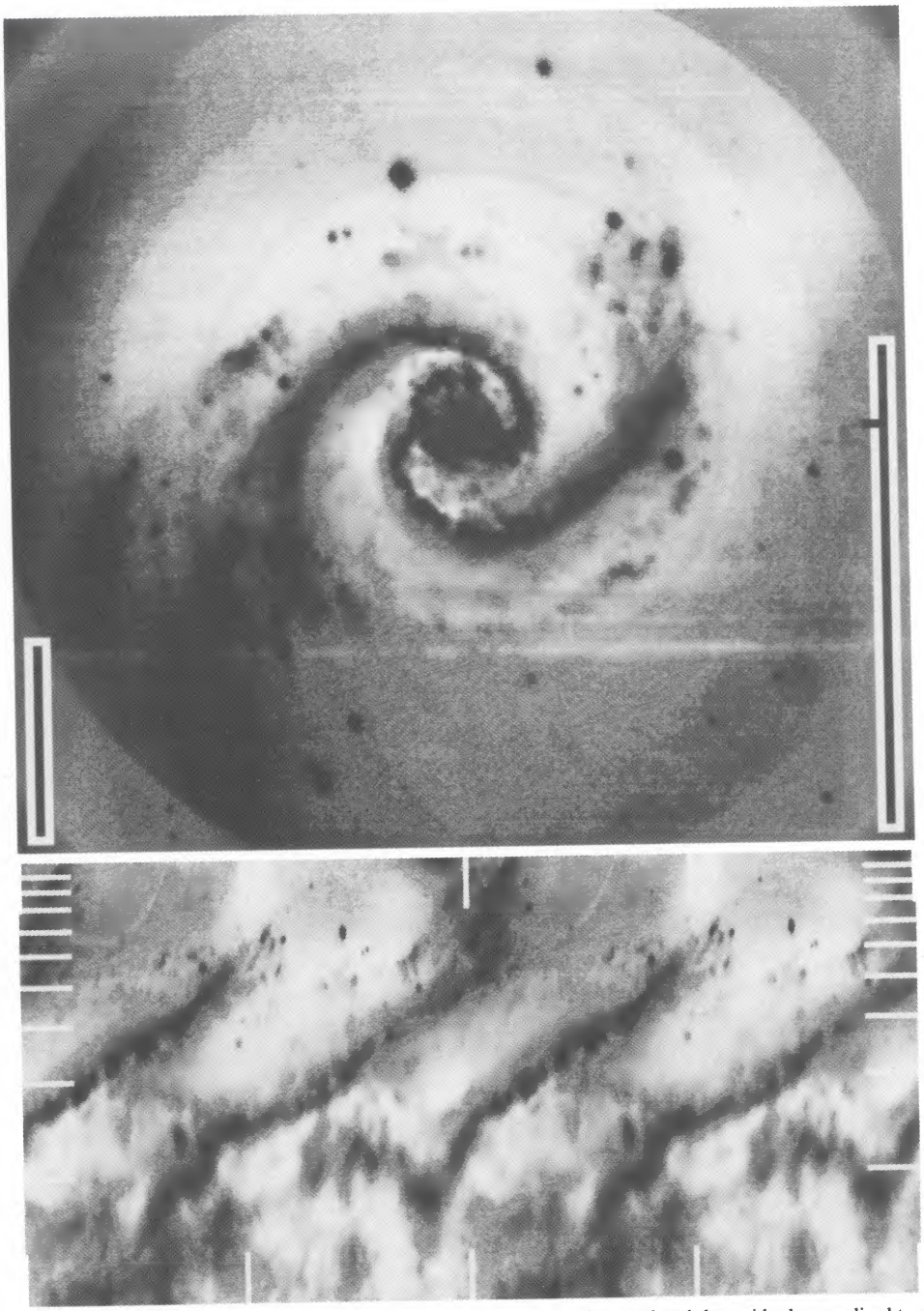

FIG. 1.—Top: NGC 1566 rectified to a face-on orientation and with the average radial profile subtracted and the residual normalized to a constant rms deviation in each concentric circle around the center. The original picture is from p. 33 in Sandage and Bedke (1988), photographed with a video camera to make a digitized 512 × 480 image. Calibration bars represent R_{25} (*right*) and 100 pixels (*left*). North is approximately to the right. Bottom: Azimuthal angle vs. log-radius plot of the enhanced image on the top. Azimuthal angle increases from left to right starting at $-180°$, with tic marks at each 180°, measured relative to the northern major axis of the galaxy and increasing counterclockwise. Radius increases from bottom to top logarithmically, with tic marks at each $0.1\,R_{25}$, from $0.1\,R_{25}$ to $0.9\,R_{25}$. The inner region ($R < 0.1\,R_{25}$) is washed out in the original atlas photograph in Sandage and Bedke.

© American Astronomical Society • Provided by the NASA Astrophysics Data System

1990ApJ...355...52E

was made with a position angle of 21° counter-clockwise from north and an inclination of 30° (de Vaucouleurs 1973).

A schematic diagram of the most prominent features in NGC 1566 is shown in Figure 2, along with the identifications discussed below (S = spur, K = kink, etc.). This diagram was traced from the photograph on page 43 of SB, and is not deprojected.

For the galactic features shown in the figures and discussed below, Table 1 gives the apparent radii in arcsecs, R_{app}, and the position angles, θ, in degrees counterclockwise from north. Also given are the deprojected radii, R_{dep}, and the ratios of these radii to R_{25} for comparison with Figure 1, and to R_{CR}, the assumed corotation radius (= 100″), for comparison with Figure 4, below. The suggested resonance radii and expected ratios R/R_{CR} at these resonances are also given, as discussed below.

The results of Fourier analysis of the digitized image of NGC 1566 are in Figure 3. The relative amplitude and phase of the symmetric part of the spiral are shown as a function of radius. The relative amplitude is defined to be the ratio (arm − interarm)/(arm + interarm), and is determined from the Fourier components as $\sum_{i=0}^{i=3} F_{4i+2}/\sum_{i=0}^{i=4} F_{4i}$. Three scales are

TABLE 1

FEATURES AND SUGGESTED RESONANCES IN NGC 1566

Feature	R_{app}	θ	R_{dep}	R/R_{25}	R/R_{CR}	Resonances	R/R_{CR} at Resonances
Inner extents of spirals							
South	9″	170°	10″	0.04	0.10	...	...
West	11	270	13	0.05	0.13	...	...
Inner kinks in spirals							
North	34	0	34	0.15	0.34	ILR	0.2–0.4
South	37	210	38	0.16	0.38	ILR	0.2–0.4
Outer extents of bar							
North	40	7	40	0.17	0.40	ILR	0.2–0.4
South	40	187	40	0.17	0.40	ILR	0.2–0.4
Spurs, average radii							
West 1	65	230	68	0.29	0.68	6:1	0.7–0.8
West 2	65	276	75	0.32	0.75	6:1	0.7–0.8
East	59	70	64	0.28	0.64	4:1	0.6–0.7
Middle kinks in spirals							
West	52	290	59	0.25	0.59	4:1	0.6–0.7
East	54	135	63	0.27	0.63	4:1	0.6–0.7
Outer extents of SF ridges							
North	90	345	95	0.41	0.95	CR	1.0
South	62	160	66	0.28	0.66		
Outer extents of smooth, continuous spirals							
North	107	16	107	0.46	1.07	CR	1.0
South	90	197	90	0.39	0.90	CR	1.0
Circle of SF							
North	112	21	112	0.48	1.12	CR	1.0
South	112	201	112	0.48	1.12	CR	1.0
East	84	111	97	0.42	0.97	CR	1.0
West	90	291	104	0.45	1.04	CR	1.0
Outer edges of smooth disk							
North	140	21	140	0.60	1.40	...	...
South	140	201	140	0.60	1.40	...	...
East	103	111	119	0.51	1.19	...	...
West	112	291	130	0.56	1.30	...	...
Arms meet outer ring							
North	168	40	171	0.74	1.71	OLR	1.5–1.8
South	168	220	171	0.74	1.71	OLR	1.5–1.8
South a	202	200	202	0.87	2.02	(SF patch)	...
South b	211	225	217	0.93	2.17	(SF patch)	...
Axes of outer ring							
North major	178	21	178	0.76	1.78	OLR	1.5–1.8
South major	215	201	215	0.92	2.15	OLR	1.5–1.8
East minor	243	111	281	1.21	2.81	Outer 1:1	2–3
West minor	206	291	238	1.02	2.38	Outer 1:1	2–3

© American Astronomical Society • Provided by the NASA Astrophysics Data System

1990ApJ...355...52E

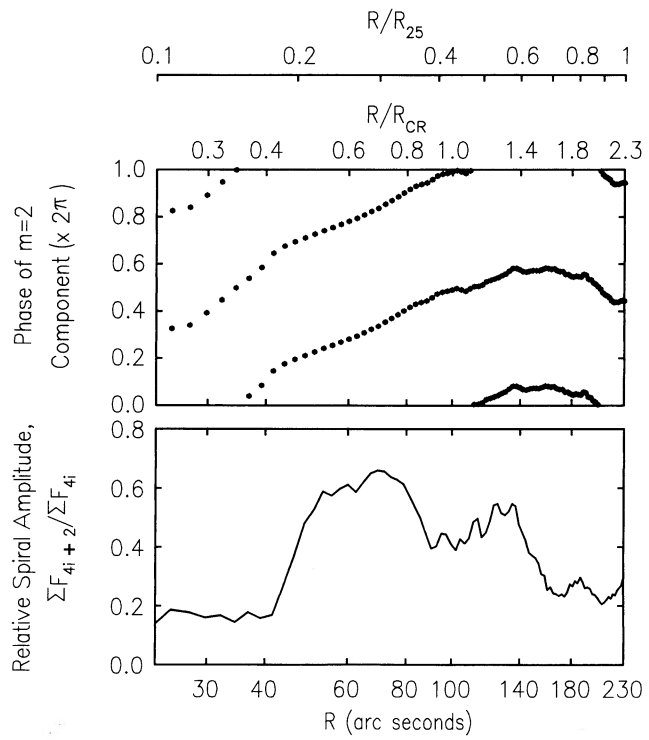

FIG. 3.—The relative amplitude of the two-armed spiral and the phase of the $m = 2$ Fourier component are plotted as a function of radius in arcsecs on the bottom coordinate axis and in units of the radius at 25th magnitude per arcsec^2 surface brightness ($R_{25} = 233''$) and the proposed radius of corotation ($R_{CR} = 100''$) at the top.

given for the abscissa: R is in arcsec on the bottom; R/R_{25} and R/R_{CR} are on the top for comparisons with Figures 1 and 4 (below), respectively.

Figure 1, which is deprojected, shows a generally circular inner structure with kinks in the inner spiral arms at an arm-center deprojected radius of 34″ to 38″. The inner bar radius from Hackwell and Schweizer (1983) is approximately the same, ~40″. This is also the radius where the relative amplitude of the spiral begins to increase in Figure 3. The inner extent of the spirals appears to be $R/R_{25} \approx 0.04$ or $R \approx 10''$ deprojected, from page 43 in SB. We suggest that an inner Lindblad resonance, if there is one, is either inside the inner spiral extent, as in M81, or close to the location of the arm kinks and bar ends. Other evidence discussed below supports the latter possibility.

The radial extents of the two spiral arm star-formation ridges are noticeably different from each other on the deprojected image (these ridges appear more similar on the SB image). The longest of these two ridges, ending in the north at 95″ deprojected radius, should terminate close to the corotation resonance if the density wave triggers this star formation. The shorter star-formation ridge, ending in the southeast at 66″ deprojected radius, smoothly continues to ~90″ with a small amount of star formation. Beyond ~100″, both spiral arms become broader, or split into pieces. There is also a thin circle of small star-formation sites that goes around the galaxy at a radius of 100″–110″; this is evident on both images in Figure 1. Such a circle also occurs in M100 near the corotation resonance, and is presumably the result of star formation independent of the density wave (EES). Thus our solution for the resonances places corotation at $R_{CR} \approx 100'' \pm 10''$.

Spiral arm spurs, best seen in the image on page 33 in SB, have inner radii of 57″ and 64″ in the west and 46″ in the east, and outer radii of 80″ and 86″ in the west and 83″ in the east (deprojected). The average radii are 68″, 75″ (west) and 64″ (east), respectively. The one in the east is the brightest and largest. These spurs will be placed at the 6:1 (west) and 4:1 (east) resonances in what follows (e.g., EES; Shu, Milione, and Roberts 1973). At the 4:1 resonance, a single spur is expected where the gas shocks upon completion of one epicyclic orbit at one-half of the way from one arm to the next. We suggest that this accounts for the large spur in the east. Two adjacent parallel spurs are expected at the 6:1 resonance because there the time between arms equals three epicyclic periods and two equally spaced shocks should occur. We suggest that this accounts for the two parallel spurs in the west. We suspect that the average radii of the spurs will be close to the resonance radii.

The spiral arms also have slight kinks midway along their lengths, at ~60″ deprojected. These are evident from Figure 1 (*bottom*) and from the top panel of Figure 3 at $R \approx 0.25\ R_{25}$. The kinks are such that the arms on either side of the kink have a higher pitch angle than the arms in the region of the kink. Because such kinks also appear in M81 near the proposed 4:1 resonance, and because identical kinks appear in theoretical studies of wave modes at the minimum amplitude points of the interference pattern near the 4:1 resonance (C. C. Lin and S. A. Lowe, 1989 private communication), we identify such kinks here with the vicinity of the 4:1 resonance. Note that the 4:1 resonance kinks are on the arms, but the 4:1 resonance spur discussed above is between the arms at the same radius.

The outer limit of the smooth stellar disk is ~140″ in the north and south and 125″ in the east and west (these would be the same sizes if the inclination angle were 50° instead of 30°). Large star-formation patches near the outer ring in the southwest appear to extend the arms to ~200″ for the inner patch and ~220″ for the outer patch. The arms or disk appear to join the inner radius of the ring in both the north and south at ~170″. If NGC 1566 is like M51, M81, and M100, which have no obvious outer ring, then the outer Lindblad resonance in NGC 1566 should be located at, or slightly beyond the 140″ to 170″ spiral-disk limit. This will be assumed below. The midpoints of the outer ring have deprojected radii of ~180″ (N), 215″ (S), 280″ (E), and 240″ (W) along the major and minor axes, respectively. If the ring is coplanar with the main optical disk, the ring is elongated perpendicular to the projected optical axis of the inclined disk.

In summary, we postulate on the basis of spiral arm morphology alone, that the inner Lindblad resonance in NGC 1566 is either at or inside the inner part of its spiral structure, possibly associated with an inner bar and spiral arm kink, that the 4:1 and 6:1 resonances are near the average radii of spurs and other kinks in the spiral arms, that the corotation resonance is near the end of the bright star-forming ridges and dust lanes and at a circle of star formation, and that the outer Lindblad resonance is near the outer extent of the arms, possibly connected with or inside the outer ring-like structure. Now we compare the relative radii of these features with the ratios of radii expected from theoretical rotation curves.

III. RATIOS OF RESONANCE RADII FROM PLAUSIBLE ROTATION CURVES

For a rotation curve, or a piece of a rotation curve, of the form $V(R) \propto R^{\alpha}$, the ratio of a resonance radius R_{res} to the

© American Astronomical Society • Provided by the NASA Astrophysics Data System

1990ApJ...355...52E

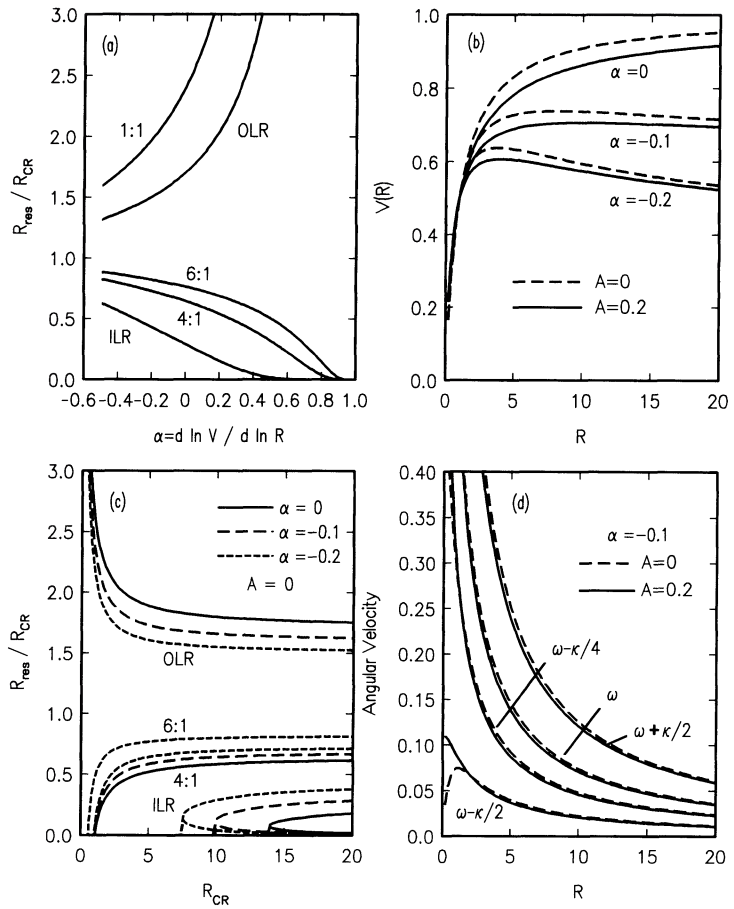

FIG. 4.—(*a*) Ratios of the indicated resonance radii to the corotation radius are plotted as a function of the power for a power law rotation curve. (*b*) Theoretical rotation curves for a two-power law model (eq. [2]), with powers A and α governing the curvature at small and large radii, respectively. (*c*) Ratios of indicated resonance radii plotted as a function of the dimensionless corotation radius for $A = 0$ and three values of α. The 6:1 resonance has curves very similar to the 4:1 resonance, and only one solution for the 6:1 resonance is shown. (*d*) Sums and differences between the angular rotation rate and integer fractions of the epicyclic frequency are shown for an illustrative case. Curves such as these were used to determine (by computer) the resonance locations plotted in panel (*c*).

corotation radius R_{CR} is

$$\frac{R_{res}}{R_{CR}} = \left(1 - \frac{2}{m}\left[\frac{1+\alpha}{2}\right]^{1/2}\right)^{1/(1-\alpha)}, \quad (1)$$

where $m = 2$ at the inner Lindblad resonance (ILR), $m = -2$ at the outer Lindblad resonance (OLR), $m = -1$ at the outer 1:1 resonance, and $m = 4$ and 6 at the inner 4:1 and 6:1 resonances. These ratios R_{res}/R_{CR} are shown in Figure 4(*a*).

A more general representation of rotation curves is

$$V(R) = \frac{R}{R^A + R^{1-\alpha}}, \quad (2)$$

for small parameters A and α. This form has a nearly solid-body rising part ($V \propto R^{1-A}$) at small R and a nearly flat part ($V \propto R^{\alpha}$) at large R. The radius is normalized to the approximate turnover radius between rising and flat parts, and the velocity is normalized to twice its value at this fiducial radius. Example rotation curves are shown in Figure 4(*b*) for $A = 0$ and 0.2, and $\alpha = -0.2$, -0.1, and 0. Comparison with real rotation curves suggests that this is a likely range for A and α, although the overall form is relatively insensitive to A, which primarily affects the ILR.

Equation (2) was used to solve for ω, $\omega + \kappa/2$, $\omega - \kappa/2$, $\omega - \kappa/4$, and $\omega - \kappa/6$ as functions of R; examples are shown in Figure 4(*d*) ($\omega - \kappa/6$ is very similar to $\omega - \kappa/4$ and is omitted from the figure for clarity). These angular rates were then used to determine the ratios of the resonance radii, R_{res}/R_{CR} for various values of the normalized corotation radius. The result is in Figure 4(*c*), which shows only the case $A = 0$ for clarity; other A values do not change the results significantly. The 6:1 resonance in Figure 4(*c*) lies on a sequence of three lines running parallel to and slightly above the three 4:1 resonance solutions (see Fig. 4[*a*]), but only the $\alpha = -0.2$ solution is shown for clarity. Note that Figure 4, (*a*) and (*c*) give the same results at large R_{CR} for the same values of α, but panel (*c*) is more appropriate at small R_{CR}, and it also gives two inner Lindblad resonances in some cases, as is appropriate for some galaxies. Equation (2) gives only one inner Lindblad resonance if A is large (e.g., 0.2).

IV. APPLICATIONS TO THE RESONANCE RADII IN NGC 1566

Now we compare these theoretical ratios of resonance radii to the observations of NGC 1566. Assuming for the moment that corotation is at $R_{CR} = 100''$, as discussed above, the inner extent of the spiral is at $\sim 0.1\ R_{CR}$, the inner spiral arm kink is at $\sim 0.36\ R_{CR}$, and the end of the bar is at $\sim 0.4\ R_{CR}$. According

© American Astronomical Society • Provided by the NASA Astrophysics Data System

1990ApJ...355...52E

to Figure 4(*c*), the second and third of these features could be near, or slightly outside, the ILR, depending on details of the rotation curve at small radii (i.e., depending on A). For $A = 0$, an ILR at $\sim 0.4\ R_{CR}$ requires a falling rotation curve in the outer part ($\alpha = -0.2$); such low values of α give small pattern speeds and large ILRs for a given value of R_{CR} in dimensionless units. Of course, there may not be an inner Lindblad resonance at all if A or R_{CR} are small.

Assuming again that $R_{CR} = 100''$, the relative size of the average radius of the two western spurs is $0.72\ R_{CR}$, which is reasonable for a 6:1 resonance according to Figure 4 (*a*) and (*c*). The average radius of the large spur in the east is $0.64\ R_{CR}$ which could be the 4:1 resonance. The middle kinks in the arms, at $\sim 0.6\ R_{CR}$, could also be near the 4:1 resonance.

The relative size of the outer spiral arm extent and the smooth disk component is between $1.4\ R_{CR}$ if the large star-formation patches in the south are not included, and $2.0\ R_{CR}$ or $2.2\ R_{CR}$ if the inner or outer patch are included (for $R_{CR} = 100''$). Neither of these are particularly good fits to the OLR solutions in Figure 4. The inner radius of the ring at $170'' = 1.7\ R_{CR}$ could be very close to the OLR, however; there the ring meets the outer part of the spiral arms in the north and south. The outer part of the ring, on the eastern and western major axes of the deprojected ellipse, is much too large to be near the OLR for this corotation radius. The outer radius of the ring lies at $\sim 2.6\ R_{CR}$, which places it close to the outer 1:1 resonance radius ($m = -1$ in Eq.[1]) for an approximately flat rotation curve (see $\alpha = 0$ in Fig. 2[*a*]). Thus the outer ring may lie between the OLR and the outer 1:1 resonance of the spiral.

An outer ring located at the outer Lindblad resonance, or between the outer Lindblad and 1:1 resonances, suggests that the ring may be a collection of stars moving semicoherently around the galaxy in a precessing epicyclic ellipse that is in phase with the inner spiral wave mode. The elongation of the ellipse, perpendicular to the current major axis of the average spiral arm potential, is probably significant. This proposed association between the outer Lindblad resonance and a ring is consistent with general theoretical discussions (Lindblad 1955; see review in Buta 1984). We are aware of no theoretical predictions of the effect of a -1:1 resonance on outer rings, although Petrou and Papayannopoulos (1986) discussed elongated orbits at the inner 1:1 resonance as an explanation for galaxy bars.

In summary, the assumption that corotation lies near the ends of the bright star-forming arms and near the circle of interarm star formation ($R_{CR} = 100''$) places the ILR near the position of a kink in the spiral arms, at the end of a bar, and outside the inner extent of the spirals. This is consistent with numerical gas flow studies in barred potentials, which show kinks and sudden velocity transitions at inner Lindblad resonances (Sanders and Huntley 1976; Athanassoula 1988). It places the 6:1 resonance at the average radius of each spur in a well-separated pair of spurs in the west, and the 4:1 resonance at the average radius of a large spur in the east. This is consistent with expected phenomena at ultraharmonic resonances (Shu, Milione, and Roberts 1973; Contopoulos and Grosbøl 1986). It also places the 4:1 resonance near the location of another kink in the arms. This is consistent with wave-mode theory of spiral structure, as shown, for example, by the solutions in Bertin *et al.* (1989) and by similar but more detailed analyses of this effect by Lin and Lowe (1989, private communication). It also puts the OLR at the outer extents of the spirals, where they meet the inner extent of the outer ring. This is consistent with the theoretical expectation that stellar spiral wave modes exist primarily inside their outer Lindblad resonances (Lin and Shu 1967; see also Toomre 1977). It is also consistent with discussions in Buta (1984), which suggest that outer rings in spiral galaxies might be associated with outer Lindblad resonances. The outer extent of the ring in NGC 1566 may also be near the outer 1:1 resonance, depending on the rotation curve.

Other solutions for the resonance locations should be considered. Comte (1983) proposed that corotation is at 130″ where the main inner spiral and smooth disk vanish. This was combined with a rising rotation curve fitted to the velocity data (Comte and Duquennoy 1982), which has a large uncertainty in the outer parts, to place the OLR at 300″ to 350″, near the outermost H II region; the ILR was placed at $\sim 35''$, as in the present analysis. Pasha (1985) proposed for NGC 1566 that corotation is at 66″, which is near the end of the bright star formation ridge in the south. In this case, the inner spiral kink and bar would end near the 4:1 resonance, the spurs and middle spiral kinks would be near corotation, and the larger star formation ridge, the ring of star formation, and the outer extent of the smooth part of the spirals would end near the outer Lindblad resonance. The smooth disk and outer ring would extend far beyond any principle resonances. Contopolous and Grosbøl (1986, 1988), on the other hand, proposed that galactic spirals may end at the 4:1 resonance. If this resonance is near the outer extent of the spiral in NGC 1566, at $\sim 100''$ for example, then corotation ($\sim 160''$) would be near the inner part of the ring, at the outer limit of the smooth disk, and the outer Lindblad resonance ($\sim 260''$) would be near the outer extent of the ring. The inner Lindblad resonance is at approximately one-half of the radius of the 4:1 resonance ($\sim 50''$) which could place it slightly outside the inner kink and bar in this case, depending on the exact rotation curve.

These other solutions are plausible. The preferred solution given here ($R_{CR} \approx 100''$) places emphasis on the spurs as tracers of ultraharmonic resonances and on the circle of star formation as a tracer of corotation. These features, in addition to the spiral arm kinks, are relatively small in radial extent and so precisely define positions in the galaxy. Unfortunately they are also relatively weak in the optical image. The other features used to indicate resonances, such as rings, bars, star-formation ridges, and so on, are more easily observed in most cases, but they define radii less precisely, and some of them are not uniquely associated with specific resonances. Thus there is some ambiguity, but we believe the preferred solution gives the most complete agreement between optical features and theoretical expectations for what happens at resonances.

We are grateful to W. Krakow for assistance with the video camera and software that were used to extract a digitized image of the published photograph of NGC 1566. We are also grateful to P. E. Seiden for assistance with the galaxy rectification software. Helpful comments by C. C. Lin and S. A. Lowe on the modal theory of spiral structure and the nature of resonances are gratefully acknowledged. D. M. E. was partially supported by a Fullam/Dudley award from the Dudley Observatory.

© American Astronomical Society • Provided by the NASA Astrophysics Data System

1990ApJ...355...52E

REFERENCES

Athanassoula, E. 1988, in *International School and Workshop in Plasma Astrophysics*, preprint.
Bertin, G., Lin, C. C., Lowe, S. A., and Thurstans, R. P. 1989, *Ap. J.*, **338**, 78.
Buta, R. 1984, Ph.D. thesis, University of Texas.
Cepa, J., and Beckman, J. E. 1990, *Ap. J.*, **349**, 497.
Comte, G. 1983, in *IAU Symposium 100, Internal Kinematics and Dynamics of Galaxies*, ed. E. Athanassoula (Dordrecht: Reidel), p. 151.
Comte, G., and Duquennoy, A. 1982, *Astr. Ap.*, **114**, 7.
Contopoulos, G., and Grosbøl, P. 1986, *Astr. Ap.*, **155**, 11.
———. 1988, *Astr. Ap.*, **197**, 83.
de Vaucouleurs, G. 1973, *Ap. J.*, **181**, 31.
de Vaucouleurs, G., de Vaucouleurs, A., and Corwin, H. G., Jr. 1976, *Second Reference Catalogue of Galaxies* (Austin: University of Texas).
Elmegreen, B. G. 1985, in *Birth and Evolution of Massive Stars and Stellar Groups*, ed. W. Boland and H. van Woerden (Dordrecht: Reidel), p. 227.
———. 1987*a*, in *IAU Symposium 115, Star-forming Regions*, ed. M. Peimbert and J. Jugaku (Dordrecht: Reidel), p. 457.
———. 1987*b*, *Ap. J.*, **312**, 626.
———. 1989, in *Galactic Models* ed. J. R. Buchler, S. T. Gottesman, and J. H. Hunter, in press.
Elmegreen, B. G., and Elmegreen, D. M. 1983, *M.N.R.A.S.*, **203**, 31.
———. 1986, *Ap. J.*, **311**, 554.
Elmegreen, B. G., Elmegreen, D. M., and Seiden, P. E. 1989, *Ap. J.*, **343**, 602.
Grosbøl, P. 1989, in *Galactic Models*, ed. J. R. Buchler, S. T. Gottesman, and J. H. Hunter, in press.
Guiderdoni, B. 1987, *Astr. Ap.*, **172**, 27.
Hackwell, J. A., and Schweizer, F. 1983, *Ap. J.*, **265**, 643.
Howard, S., and Byrd, G. G. 1990, *A.J.*, submitted.
Hunter, D. A., and Gallagher, J. S. III. 1986, *Pub. A.S.P.*, **98**, 5.
Kennicutt, R. C. 1981, *A.J.*, **86**, 1847.
———. 1989, *Ap. J.*, **344**, 685.
Kent, S. M. 1987, *A.J.*, **93**, 1062.
Lin, C. C., and Lowe, S. A. 1989, in *Galactic Models*, ed. J. R. Buchler, S. T. Gottlesman, and J. H. Hunter, in press.
Lin, C. C., and Shu, F. H. 1967, in *IAU Symposium 31, Radio Astronomy and the Galactic System*, ed. H. van Woerden (New York: Academic Press), p. 313.
Lindblad, B. 1955, *Stockholm Obs. Ann.*, **18**, No. 6.
Lubow, S. H. 1986, *Ap. J. (Letters)*, **307**, L39.
Lubow, S. H., Balbus, S. A., and Cowie, L. L. 1986, *Ap. J.*, **309**, 496.
McCall, M. L., and Schmidt, F. H. 1986, *Ap. J.*, **311**, 548.
Pasha, I. I. 1985, *Astr. Tsirk.*, **1387**, 4.
Petrou, M., and Papayannopoulos, T. 1986, *M.N.R.A.S.*, **219**, 157.
Roberts, W. W. 1969, *Ap. J.*, **158**, 123.
Roberts, W. W., Roberts, M. S., and Shu, F. H. 1975, *Ap. J.*, **196**, 381.
Roy, J.-R., Belley, J., and Walsh, J. R. 1989, *A.J.*, **97**, 1010.
Sandage, A., and Bedke, J. 1988, *Atlas of Galaxies* (Washington, DC: US GPO).
Sersic, J. L., and Calderon, J. H. 1978, *Pub. Dept. Astr. Univ. Chile*, **3**, 55.
Sanders, R. H., and Huntley, J. M. 1976, *Ap. J.*, **209**, 53.
Shu, F. H. 1985, in *IAU Symposium 106, The Milky Way Galaxy*, ed. H. van Woerden, R. J. Allen, and W. B. Burton (Dordrecht: Reidel), p. 530.
Shu, F. H., Milione, V., and Roberts, W. W. 1973, *Ap. J.*, **183**, 819.
Thronson, H. A., Tacconi, L., Kenney, J., Greenhouse, M. A., Margulis, M., Tacconi-Garman, L., and Young, J. 1989, *Ap. J.*, **344**, 747.
Toomre, A. 1977, *Ann. Rev. Astr. Ap.*, **15**, 437.
Tremaine, S., and Weinberg, M. D. 1984, *Ap. J. (Letters)*, **282**, L5.

BRUCE G. ELMEGREEN: IBM Research Division, T. J. Watson Research Center, P.O. Box 218, Yorktown Heights, NY 10598

DEBRA MELOY ELMGREEN: Vassar College Observatory, Poughkeepsie, NY 12601

© American Astronomical Society • Provided by the NASA Astrophysics Data System